Sensorless Switched Reluctance Motor Drive With Torque Ripple Minimization

Hoe S. Ooi and Tim C. Green
Department of Electrical and Electronic Engineering
Imperial College of Science, Technology and Medicine
London SW7 2BT, United Kingdom

Abstract — Position sensorless torque ripple minimization techniques are presented to deal with the issues of rotor position sensor requirement and high torque ripple production in a switched reluctance motor (SRM) drive. In the proposed methods, multilayer perceptron (MLP) neural networks have been applied to learn the non-linear electrical characteristics of an SRM. The non-linear model of an SRM is used in the simulation which takes into account the magnetisation saturation effect. The model is verified with experimental flux linkage, inductance and torque data taken from a 7.5kW SRM. Simulation results have shown that torque ripple minimization can be achieved without a rotor position sensor or torque sensor. Experimental work has been undertaken to show the effectiveness of the torque prediction by the neural network.

INTRODUCTION

The Switched Reluctance Motor has received much attention for development of various general-purpose adjustable speed drives in industrial and consumer product applications. The SRM is simple in construction and can operate at high speeds. The simple power electronic converter requirement and fault tolerance capability are among other specific advantages of SRM drives. Alongside the advantages, SRM exhibits two main disadvantages of requiring a rotor position sensor for its operation and producing high torque ripple. The position sensor is a significant contribution to the cost and complexity, and tends to reduce the reliability of the drive system. The origin of the torque ripple in an SRM is the highly non-linear and discrete nature of the torque production mechanism. The torque ripple is significant at the commutation instant.

The literature reports both sensorless [1], [2], [3], [4], [5], [6], [7] and torque ripple minimization [8], [9], [10], [11], [12], [13], [14] methods for SRM but the challenge is to achieve these together. The aim of this work is to provide a unified solution. The work presented here begins with a description of the 12/8 SRM model used and the verification of this model with experimental measurement. This will be followed by two proposed sensorless torque ripple minimization methods namely a Single Neural Network (SNN) scheme and a Dual Neural Network (DNN) scheme. The simulation carried out in Matlab and the results will be presented to show the success of the proposed methods. Experimental work has been undertaken to show the effectiveness of the torque prediction by the neural network.

SIMULATION MODEL AND EXPERIMENTAL MEASUREMENTS

The model of the SRM used in the simulation was based on a trigonometric function for the variation of the unsaturated inductance with the rotor position and a hyperbolic function for saturation approximation [15]. Because SRM are designed to work in saturation, linear models are unacceptable and although the saturation model here is an approximation, its results are realistic enough for a system level simulation. Figure 1 shows the graphs of flux linkage, inductance and electromagnetic torque plotted against rotor position for both the simulation model (left) and static measurements (right). The experimental flux linkage data was calculated based on the measured phase voltage and current with the rotor locked at various positions over the rotor pole pitch. The phase inductance was determined from the rate of change of the calculated flux linkage. Two sets of experimental torque data were produced. The first set was calculated based on the co-energy produced by the flux linkage and the second set was measured by a load cell. Figure 1a shows that the simulation model has produced a sufficiently accurate flux linkage characteristic. The phase inductance in Figure 1b produced by the simulation model shown a lower saturation level at high current compared to the experimental data. The torque produced by the simulation model shows a larger deviation than that of the flux linkage and phase inductance simulation data. Despite the differences produced by the simulation model, it has produced a characteristic that resemble the characteristic of an SRM and can be used to assess the sensorless control methods.

0-7803-5692-6/00/$10.00 (c) 2000 IEEE

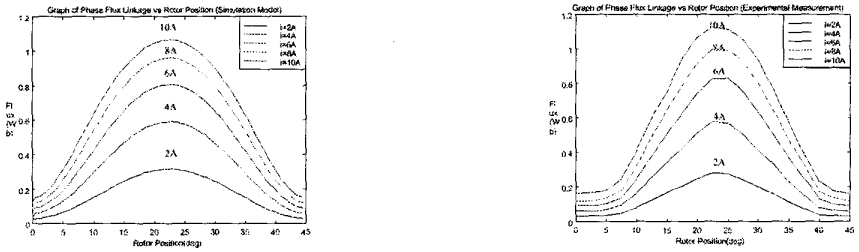

Fig. 1a. Graph of Flux Linkage against Rotor Position (simulation model and experimental measurement)

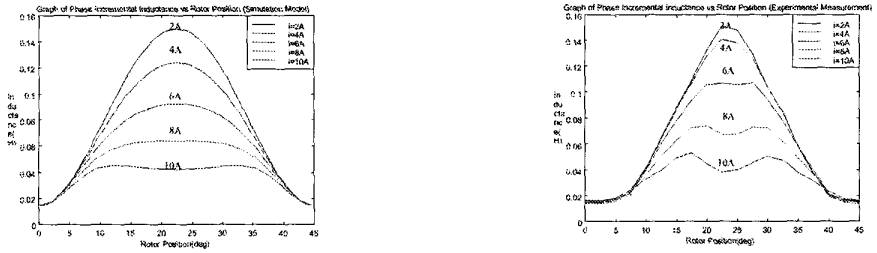

Fig 1b. Graph of Inductance against Rotor Position (simulation model and experimental measurement)

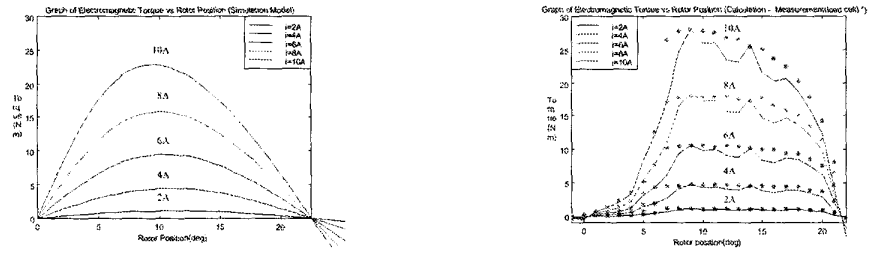

Fig 1c. Graph of Electromagnetic Torque against Rotor Position
(simulation model, experimental measurement and calculation from co-energy term)

PROPOSED SENSORLESS TORQUE RIPPLE MINIMISATION METHODS

Two methods are proposed here for sensorless torque ripple minimization. In both, an artificial neural network has been used to learn the non-linear electromagnetic characteristic of an SRM. Neural networks are suitable for these applications because of their ability to learn a non-linear input-output function of a system by observing a set of input-output examples (training set) of that system.

A. SNN Scheme

In the SNN scheme, the control model comprises a neural network representing the electrical characteristic and a linear observer used as an estimator for the mechanical system. As will be shown in this section, the speed and position state errors need for the estimator can be obtained from the flux linkage prediction neural network.

A 2-layer MLP neural network is chosen and trained in off-line mode to predict the flux linkage ψ of a phase of an SRM with the phase current i and rotor position θ as its inputs. The parameters of the trained flux linkage prediction neural network i.e. the weights and biases, are used to obtain information on the incremental inductance $\partial\psi/\partial i$, the partial derivative of flux linkage with respect to rotor position $\partial\psi/\partial\theta$, the partial derivative of incremental inductance with respect to rotor position $\partial(\partial\psi/\partial i)/\partial\theta$ and the electromagnetic torque T. O'Donavan *et al.* [16] proposed using the weights and biases of the flux linkage prediction neural network to obtain the electromagnetic torque. The work presented here carries this idea further to obtain three other variables, i.e.

$\partial\psi/\partial i$, $\partial\psi/\partial\theta$ and $\partial(\partial\psi/\partial i)/\partial\theta$ which can be used with a linear observer to determine the rotor position.

The weights and biases of the flux linkage prediction neural network are manipulated to obtain $\partial\psi/\partial i$, $\partial\psi/\partial\theta$ and $\partial(\partial\psi/\partial i)/\partial\theta$ as follows

$$\psi_{NN} = \sum_{j=1}^{N} W_j \tanh\left(W_{ji} i + W_{j\theta}\theta + B_j\right) + B_o \tag{1}$$

$$\partial\psi_{NN}/\partial i = \sum_{j=1}^{N} W_j W_{ji} \operatorname{sech}^2\left(W_{ji} i + W_{j\theta}\theta + B_j\right) \tag{2}$$

$$\partial\psi_{NN}/\partial\theta = \sum_{j=1}^{N} W_j W_{j\theta} \operatorname{sech}^2\left(W_{ji} i + W_{j\theta}\theta + B_j\right) \tag{3}$$

$$\partial(\partial\psi_{NN}/\partial i)/\partial\theta = -2\sum_{j=1}^{N} W_j W_{ji} W_{j\theta} \tanh\left(W_{ji} i + W_{j\theta}\theta + B_j\right) \cdot \operatorname{sech}^2\left(W_{ji} i + W_{j\theta}\theta + B_j\right) \tag{4}$$

where N is the number of neurons in the hidden layer
W_j are the weights at the output layer
W_{ji} are the weights at the input layer connecting the input current i to the hidden neurons
$W_{j\theta}$ are the weights at the input layer connecting the input rotor position θ to the hidden neurons
B_j are the biases for the hidden neurons
B_o is the bias for the output neuron

The structure of the linear observer is shown in Figure 2 and described by the state-space equation (6). The input to the observer is the total electromagnetic torque produced by the SRM T_{total} as calculated from the neural network. The states of the observer are the estimated speed of rotation ω and rotor position θ. The observer produces rotor position at its output based on the states errors e_ω, e_θ computed using the terms in (2) – (4) and the phase currents and voltages. The computation of the observer states errors are described as follows

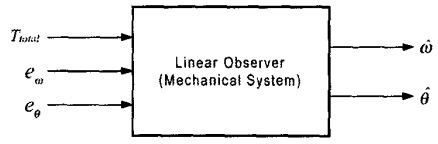

Fig 2. Structure of linear observer (mechanical system)

$$\begin{aligned} \dot{\hat{\omega}} &= 1/J\left(T_{total} - b\omega\right) \\ \dot{\hat{\theta}} &= \omega \end{aligned} \tag{5}$$

$$\begin{bmatrix} \dot{\hat{\omega}} \\ \dot{\hat{\theta}} \end{bmatrix} = \begin{bmatrix} -b/J & 0 \\ 1 & 0 \end{bmatrix} \begin{bmatrix} \hat{\omega} \\ \hat{\theta} \end{bmatrix} + \begin{bmatrix} 1/J \\ 0 \end{bmatrix} [T_{total}] + \begin{bmatrix} K_\omega \\ 0 \end{bmatrix} [e_\omega] + \begin{bmatrix} 0 \\ K_\theta \end{bmatrix} [e_\theta] \tag{6}$$

$$[\hat{\theta}] = [0 \quad 1] \begin{bmatrix} \hat{\omega} \\ \hat{\theta} \end{bmatrix}$$

where T_{total} is the total torque produced by SRM
J is the inertia of the rotor
B is the viscous damping
$\hat{\omega}$ is the estimated speed of rotation
$\hat{\theta}$ is the estimated rotor position
e_ω is the speed error
e_θ is the rotor position error

Computation of speed error:

The difference between the EMF term calculated from the observed voltage and current and that from the flux linkage prediction neural network yields an indication of the speed error as shown in (7) - (9). Equations (7) - (9) show that for a well trained flux linkage prediction neural network, speed error can be calculated by taking the difference between the derivative of the flux linkage of the phase winding and the derivative of the flux linkage from the flux linkage prediction neural network.

$$\begin{aligned} E &= (V - iR) \\ &= \frac{d\psi(i,\theta)}{dt} \\ E_{NN} &= \frac{d\psi_{NN}(i,\theta)}{dt} \end{aligned} \tag{7}$$

$$\begin{aligned} e_E &= E - E_{NN} \\ &= \frac{d\psi(i,\theta)}{dt} - \frac{d\psi_{NN}(i,\theta)}{dt} \\ &= \left(\frac{\partial\psi}{\partial i}\cdot\frac{di}{dt} + \frac{\partial\psi}{\partial\theta}\cdot\omega\right) - \left(\frac{\partial\psi_{NN}}{\partial i}\cdot\frac{di}{dt} + \frac{\partial\psi_{NN}}{\partial\theta}\cdot\hat{\omega}\right) \\ &= \left(\frac{\partial\psi}{\partial i} - \frac{\partial\psi_{NN}}{\partial i}\right)\cdot\frac{di}{dt} + \left(\frac{\partial\psi}{\partial\theta} - \frac{\partial\psi_{NN}}{\partial\theta}\right)\cdot\omega + \\ &\quad \frac{\partial\psi_{NN}}{\partial\theta}\cdot(\omega - \hat{\omega}) \end{aligned} \tag{8}$$

$$e_{\omega} \approx e_E / \frac{\partial \psi_{NN}}{\partial \theta} \qquad if \ \frac{\partial \psi}{\partial i} \approx \frac{\partial \psi_{NN}}{\partial i}$$
$$and \ \frac{\partial \psi}{\partial \theta} \approx \frac{\partial \psi_{NN}}{\partial \theta} \tag{9}$$
$$where \quad e_E = (V - iR) - \left(\frac{\partial \psi_{NN}}{\partial i} \cdot \frac{di}{dt} + \frac{\partial \psi_{NN}}{\partial \theta} \cdot \hat{\omega} \right)$$

Computation of rotor position error:

The rotor position error is calculated based on the slope of the incremental inductance curve. The error between the actual and estimated rotor position allows the gradient of the curve to be determined when the inductance at both positions are known.

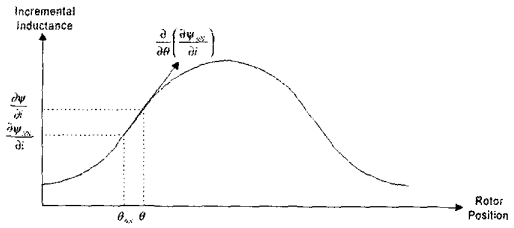

Fig 3. Computation of Position Error

$$\frac{\partial}{\partial \theta}\left(\frac{\partial \psi}{\partial i}\right)_{NN} = \frac{\frac{\partial \psi}{\partial i} - \left(\frac{\partial \psi}{\partial i}\right)_{NN}}{\theta - \theta_{NN}} \tag{10a}$$

$$e_{\theta} = \theta - \theta_{NN} = \frac{\frac{\partial \psi}{\partial i} - \left(\frac{\partial \psi}{\partial i}\right)_{NN}}{\frac{\partial}{\partial \theta}\left(\frac{\partial \psi}{\partial i}\right)_{NN}} \tag{10b}$$

The same flux linkage prediction neural network is used to calculate the torque developed by each phase of the SRM. This is used in a hysteresis controller to provide minimum torque ripple operation within the hysteresis band. The torque ripple minimization is based on a pre-defined torque waveform. The implementation of SNN scheme is shown in Figure 4.

B. DNN Scheme

In the DNN scheme, one MLP neural network is used for predicting the rotor position θ and a second is used to provide a current reference to meet the desired torque. The first neural network is chosen and trained in off-line mode to predict the rotor position θ. The inductance, L of each the stator phase is a function of the phase current i and of the rotor position θ. In order to determine the rotor position θ, the neural network is trained to learn the inverse of the function, i.e. to learn the mapping of $\theta=f(L,i)$. Since the rotor position θ is dependent on the value of the current and inductance of each phase, these parameters, i.e. i_1, i_2, i_3 and L_1, L_2, L_3 have been chosen as the inputs of the neural networks. The reference phase current produced by the second neural network is based on a pre-defined torque waveform. The current is regulated by a PI current controller. The implementation of DNN scheme is shown in Figure 5.

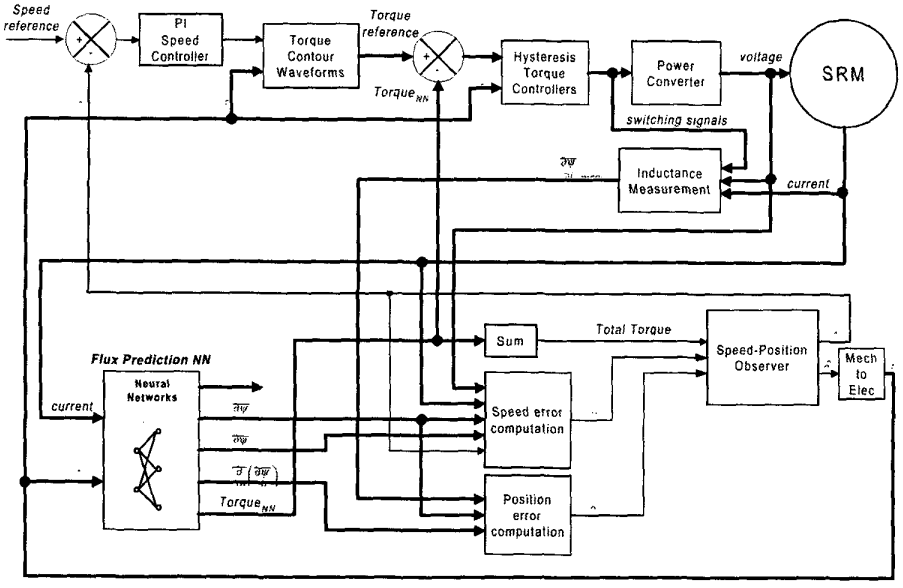

Fig 4. Single Neural Network (DNN) Scheme

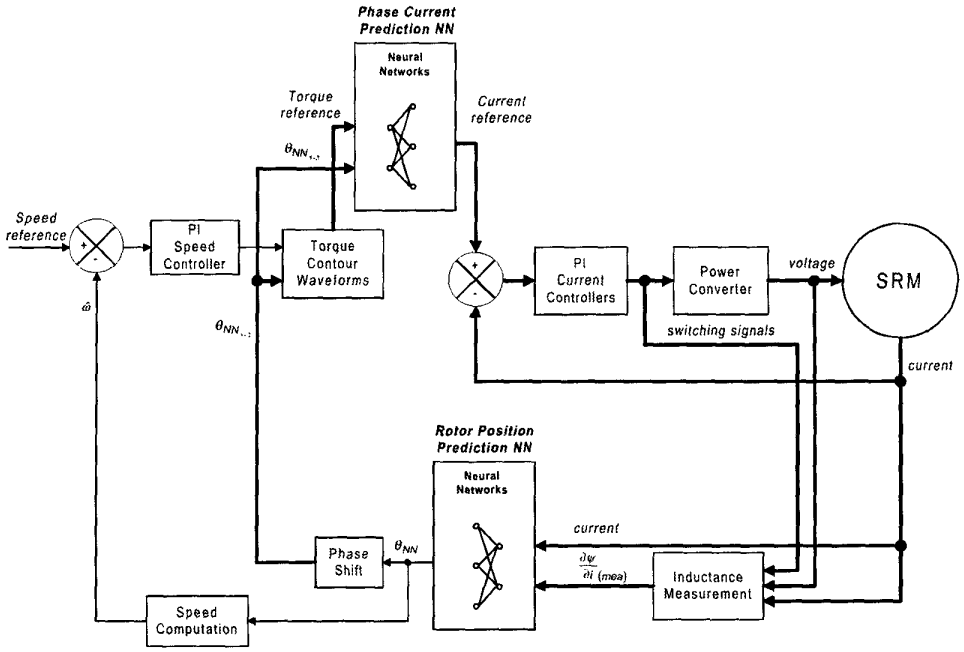

Fig 5. Dual Neural Network (DNN) Scheme

SIMULATION RESULTS

The simulation results of the proposed methods are shown in Figure 6 for a speed of rotation of 100 rad/s and a torque demand of 10Nm. The simulation was also carried out for a trapezoidal phase current as shown on the lower plot of Figure 6a. From these figures, it can be seen that the DNN scheme reduces the peak to peak torque ripple from 30% to approximately 6% as compared to trapezoidal current. The SNN scheme reduced the torque ripple to only 20%. In both of the methods, rotor position sensor is not required for the operation of SRM drive. The DNN scheme uses a separate rotor position prediction neural network to predict the rotor position. The error in the rotor position prediction is confined to whether the neural network was trained sufficiently and its resultant generalisation characteristic. In the SNN scheme, the rotor position is estimated by a linear observer with its speed and position states error computed from the flux linkage neural network. The accuracy of the states error will affect the accuracy of the estimated rotor position. Further errors may result if the observer is not based on an accurate mechanical model.

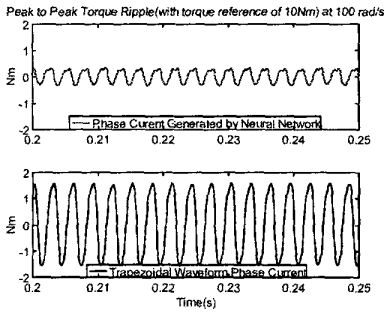

Fig 6a. SRM Drive with DNN Scheme

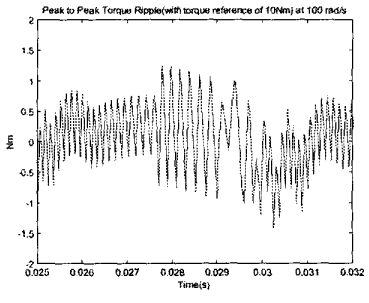

Fig 6b. SRM Drive with SNN Scheme

EXPERIMENTAL RESULTS

The simulation model has been experimentally verified by static measurement of an SRM. The experimental set-up for the SRM drive includes a fixed point DSP controller, IGBT power converter switching at 20kHz and a 12/8 SRM rated at 7.5kW (48Nm @ 1500rpm) which is configured to run in a closed loop servo control system. Q-format numbers are used to represent the binary point values of the weights and biases of the neural network. The hyperbolic tangent function is implemented using a look-up table. Experimental data was collected with a TDS380 scope and plotted in Matlab. Figure 7 shows the results of the torque prediction achieved with a 9 hidden neuron neural network. A simple current pulse demand and PI current control loop sampled at 2kHz was used for this test. The results show that the neural network is able to predict the torque with a sampling rate of 2kHz using the fixed-point DSP. A rotor position of zero corresponds to the unaligned position and the aligned position is at 22.5°. The 9 neuron hidden network has not learnt the characteristic well near the unaligned position. A greater number of neurons can improve this but at the expense of execution time.

CONCLUSIONS

The proposed methods have been shown to achieve torque ripple minimization in SRM drive without a rotor position sensor. Two methods have been proposed and tested in simulation. In simulation, the DNN scheme has shown a better performance in reducing the torque ripple compared to the SNN scheme. The peak to peak torque ripple has been reduced from approximately 30% (trapezoidal current) to 20% (SNN scheme) and to 6% (DNN scheme). The SRM model used in the simulation has been verified with experimental data taken from a 7.5kW SRM. The neural network torque prediction for the proposed method has been implemented using a fixed-point DSP and has shown satisfactorily results in predicting the torque at different current level over the rotor pole-pitch .

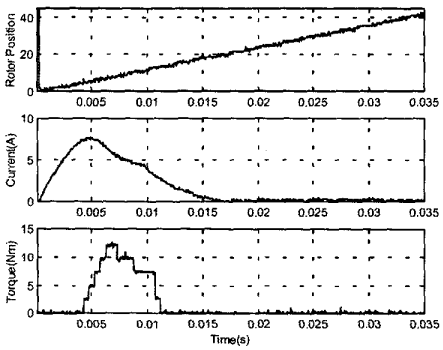

Fig 7a. Torque Prediction (7A peak)

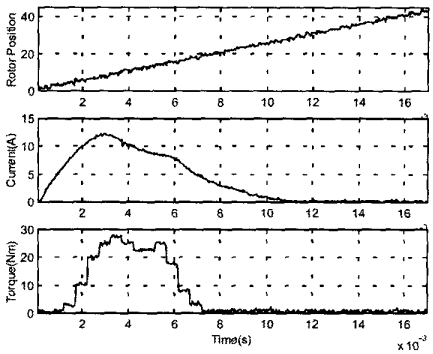

Fig 7b. Torque Prediction (12A peak)

REFERENCES

[1] P.P. Acarnley, R.J. Hill and C.W. Hooper, "Detection of rotor position in stepping and switched motors by monitoring current waveforms", IEEE Trans. Ind. Eletronics, Vol. IE-32, No.3, August 1985, pp 215-222

[2] A. Lumsdaine and J.H. Lang, "Sate observer for variable-reluctance motors", IEEE Trans. Ind. Electronics, Vol 37, No.2, April 1990, pp 133-142

[3] W.D. Harris and J.H. Lang, "A simple motion estimator for variable-reluctance motors", IEEE Trans. Ind. Applications, Vol.26, No.2, March/April 1990, pp 237-243

[4] J.P. Lyons, S.R. MacMinn and M.A. Preston, "Flux/current methods for SRM rotor position prediction", Proc. IEEE-IAS' 1991, pp 482-487

[5] S.R. MacMinn, W.J. Rzesos, P.M. Szczesny and T.M. Jahns, "Application of sensor integration techniques to switched reluctance motor drives", IEEE Trans. Ind. Applications, Vol.28, N0.6, Nov/Dec 1992, pp 1339-1344

[6] I. Husain and M. Ehsani, "Rotor position sensing in switched reluctance motor drives by measuring mutually induced voltages", IEEE Trans. Industry Applications, Vol.30, No.3, May/June 1994, pp 665-672

[7] M. Ehsani, I. Husain, S. Mahajan and K.R. Ramani, "New modulation encoding techniques for indirect rotor position sensing in switched reluctance motors", IEEE Trans. Ind. Applications, Vol.30, No.1, Jan/Feb 1994, pp 85-91

[8] R.C. Kavanagh, J.M.D. Murphy and M.G. Egans, "Torque ripple minimization switched reluctance drives using self-learning techniques", Proc. IECON 91', pp 289-294

[9] D.S. Schramm, B.W. Williams and T.C. Green, "Torque ripple reduction of switched reluctance motors by phase current optimal profiling", IEEE PESC 1992, Vol 2. Pp 857-860

[10] D.S. Reay, T.C. Green and B.W. Williams, "Application of associative memory neural networks to the control of a switched reluctance motor", Proc. IECON 93', pp 200-206

[11] C. Rochford, R.C. Kavanagh, M.G. Egan and J.M.D. Murphy, "Development of smooth torque in switched reluctance motors using self-learning techniques", EPE 1993, Vol. 6, pp 14-19

[12] K. Russa, I. Husain and M. Elbuluk, "Torque Ripple Minimization is switched reluctance machines over a wide speed range", IEEE Trans. Ind. Applications, Vol. 34, No. 5, Sep/Oct 1998

[13] C. Shang, D.S. Reay and B.W. Williams, "Commutating switched reluctance motors efficiently via CMAC neural network with learning rate function", Proc. American Ctrl. Conf., pp 237- 241

[14] P.C.Kjaer, J.J. Gribble and T.J.E. Miller, "High-grade control of switched reluctance machines", IEEE Trans. Ind. Applications, Vol. 33, No. 6, Nov/Dec 1997, pp 1585-1593

[15] H.S. Ooi and T.C. Green, "Simulation of neural networks to sensorless control of switched reluctance motor", PEVD 98', pp 281-291

[16] J.G. O'Donavan, P.J. Roche, R.C. Kavanagh, M.G. Egan, J.M.D. Murphy, "Neural network based torque ripple minimisation in a switched reluctance motor", IECON 94', pp 1226-1231